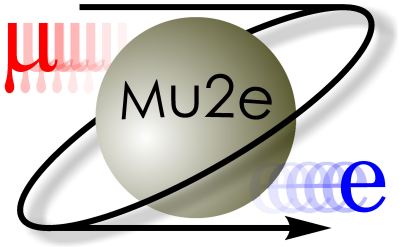


# Preliminary studies of proton reconstruction at Mu2e

Intern:
Valerio Bertacchi

Supervisor:
Pasha Murat

Co-Supervisor:
Gianantonio Pezzullo

10 October 2016

Mu2e Fermilab - Summer Student Programme 2016

Dipartimento di Fisica "E. Fermi" - Università di Pisa

**Abstract**

In this work are presented some studies that allow to use Mu2e reconstruction algorithm to reconstruct protons with modification at configuration level only and at current efficiency it is possible to reconstruct $2.90 \pm 0.06$ protons per microbunch. It is exposed a method to monitor the muon flux on the target and its fluctuations at millisecond time scale using the proton counting. Studies on proton momentum reconstruction are presented too.

# Contents

# 1 Introduction: Mu2e experiment

In the Standard Model the lepton flavour-violating (LFV) processes are forbidden, and the only experimental evidence of such processes are neutrino oscillations. Anyway Standard Model could be extended to include the neutrino LFV processes. On the other side, there are no experimental evidences of charged lepton flavour violation (CLFV), that can't be easily included in Standard Model extensions.

Mu2e experiment want to study the conversion of muons into electrons in nuclear field, without neutrinos emission:

$$\mu^- + N \to e^- + N.$$

This process is allowed by Standard Model extension that included neutrino oscillation (with a virtual neutrino loop that oscillate in the loop, like figure 1.1 ) but the branching ratio of this process in $< 10^{-50}$ for both $\mu^- \to e^-\gamma$ and $\mu^- N \to e^- N$, instead the same process could be explained by Beyond Standard Model (BSM). Mu2e experiment[2] intends to improve a single event sensibility (SES) of $2.5 \cdot 10^{-17}$ at 90% of confidence level, improving of 4 order of magnitude the current SES limit of $7 \cdot 10^{-13}$ measured by SINDRUM II experiment. So Mu2e studies has a big discovery potential, and in absence of evidence of the process the reduction of SES is an important discriminant among BSM models.

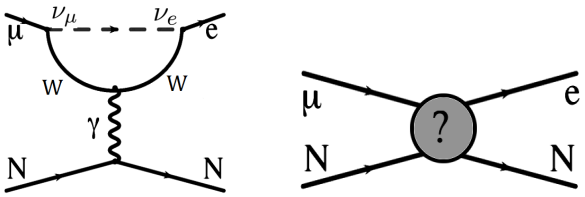


(a) (b)

*Figure 1.1: (a) muon to electron conversion by neutrino oscillation diagram and (b) CFLV process (the interaction with nucleus could be with photon or with another particle)*

## 1.1 Signal and Background of the experiment

The chosen nucleus in Mu2e experiment is aluminium, and the expected signal is a monoenergetic electron [7] with an energy of

$$E_e = m_\mu - E_b(Z) - R_N(A) = 104.97 \text{ MeV}$$

where $E_b(Z) \simeq \frac{Z^2\alpha^2 m_\mu}{2}$ is the atomic binding energy and $R_N(A) = \frac{m_m u^2}{2m_N}$ is the nuclear recoil energy, because the kinematics is the same of a two-body decay.

The muons that arrive on the target, with a flux $\phi_\mu$, could be stopped inside the target, could pass the target or could decay in flight. The stopped fraction is $f_{\text{stop}} \equiv \frac{N_{\text{stopped}}}{N_{\text{incident}}} \simeq 0.58$, so the stopped flux is $f_{\text{stop}}\phi_\mu$. The stopped muons could decay in orbit of the nucleus or could be captured from the nucleus and the ratio between captured and decayed is $R_{\text{capt}} \equiv \frac{N_{\text{capt}}}{N_{\text{dec}}} \simeq 0.6$.

The decay-in-flight muons do not contribute background because the maximum energy of the electron from muons decay (given by Michel spectrum) is 52.8 MeV, well under the signal energy window. Instead the source of background are:

- electrons from Decay-in-orbit (DIO) muons ($\mu^- N \to e^- \bar{\nu}_e \nu_\mu N$), that scale with beam intensity
- photons from radiative muon capture (RMC) ($\mu^-$Al$\to \gamma\nu_\mu$Mg), that scale with beam intensity
- antiprotons ($pp \to ppp\overline{p}$), delayed because spiral slowly down beam line
- electrons from radiative pion capture ($\pi^- N \to \gamma N^* \to e^+ e^- N^*$), prompt process coincident in time with muons
- electrons or muons that are initiated by cosmic rays
- proton from nuclear disintegration [6]
- events that result from reconstruction errors induced by additional activity in the detector from conventional processes

The DIO electrons are the most important background: if the muons is bound in atomic orbit, the outgoing electron can exchange momentum with the nucleus, resulting in an electron with a maxium possible energy, ignoring the neutrino mass, equal to the energy of a Conversion Electron (CE) of the

signal, however with very small probability. At the kinematic limit of the bound decay, the two neutrinos carry away no momentum and the electron recoils against the nucleus, simulating the two-body final state of muon to electron conversion. The differential energy spectrum of electrons from muon DIO falls rapidly as the energy approaches the endpoint, approximately as $(E_{\text{endpoint}} - E_e)^5$. In figure 1.2 is shown the spectrum in logarithmic scale.

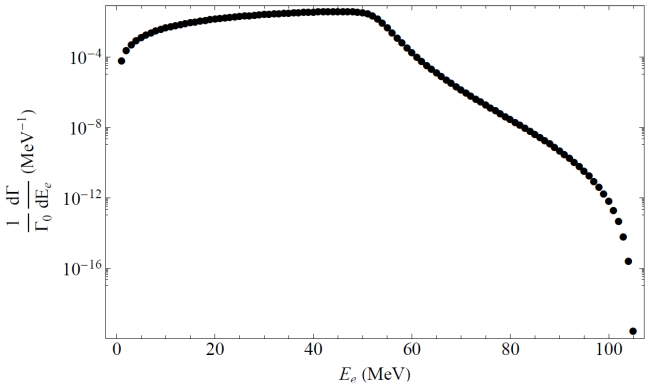


*Figure 1.2: Electron DIO energy spectrum spectrum, in logarithmic scale to show the endpoint shape in CE signal region ($\Gamma_0 = \frac{G_F^2 m_\mu^5}{192\pi^3}$, where $G_F$ is the Fermi constant. Reference: [4])*

## 1.2 Mu2e apparatus

In figure 1.3 is shown the complete apparatus of Mu2e.

An integrated array of superconducting solenoids forms a graded magnetic system that includes the Production Solenoid, the Transport Solenoid and the Detector Solenoid. The Production Solenoid contains the Production Target that intercepts an 8 GeV kinetic energy, high intensity, pulsed proton beam. The S-shaped Transport Solenoid transport slow energy $\mu^-$ from the Production Solenoid to the Detector Solenoid and allows sufficient path length for a large fraction of the pions to decay to muons. Additionally, the Transport Solenoid attenuates nearly all high energy negatively charged particles, positively charged particles and line-of-sight neutral particles. The upstream section of the Detector Solenoid houses the muon stopping target and has a graded magnetic field. The graded field increases the acceptance for conversion electrons and plays a key role in rejecting beam-related backgrounds. The downstream section of the Detector Solenoid has a nearly uniform field in the region occupied by the tracker and the calorimeter.

The tracking detector is made from low mass straw tubes oriented transverse to the solenoid axis. The momentum resolution is dominated by fluctuations in the energy lost in the stopping target and proton absorber, by multiple scattering, and by bremsstrahlung of the electron in the tracker. The calorimeter consists of about 1900 crystals arranged in two disks oriented transverse to the solenoid axis. The calorimeter provides timing and energy information important for providing a fast trigger and efficient particle identification.

In front of the detectors there is a proton absorber: a block of high-density polyethylene (HDPE) used to stop most of protons from nuclear disintegration that could make the occupancy and the charge deposition in the tracker too high.

### 1.2.1 Timing of beam signal

From the fermilab Main Injector every 1.4 seconds are acqired two proton batches, each containing $4 \cdot 10^{12}$ protons and a time distance of 43 ms. A resonant extraction system inject every 1695 ns a bunch containing $3.9 \cdot 10^6$ protons (called microbunch) into the Mu2e beamline. In figure 1.4 is shown the microbunch structure of the proton signal.

For the purpose of this work the microbunch is the fundamental signal that is treated, and so the proton signal can be considered a pulsed signal with a period of 1.7 $\mu$s. Moreover in the simulations is called "event" a proton microbunch.

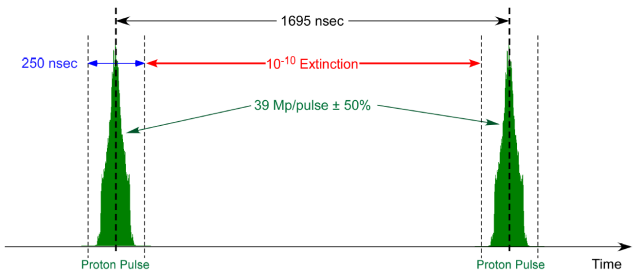


*Figure 1.4: Microbunch structure: the width of the microbunch is $\simeq 250$ ns, the time distance is chosen $\simeq 1.7$ $\mu$s tho guaratee a $10^{-10}$ signal extinction*

### 1.2.2 The tracker

The tracker is made of planes of straw tubes, orthogonal to beam line. Each plane is made of 6

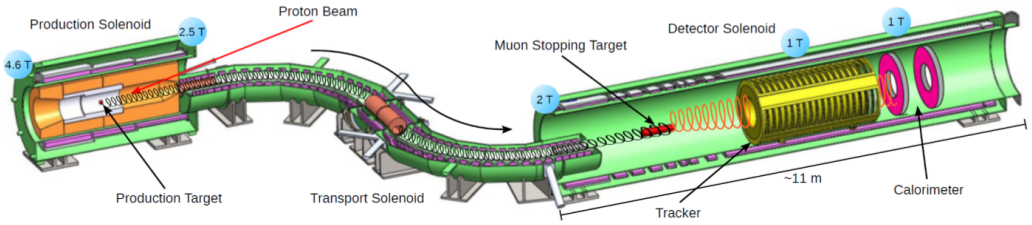


*Figure 1.3: The Mu2e apparaus*

panels of 96 tubes per panel and the entire tracker is made of 36 planes coupled in 18 stations. In each plane the six panels are disposed as in figure 1.5 to form a central hole and avoid the detection of most of DIO electrons in signal energy window (so electrons with $p_\perp \simeq 52.8$ MeV/c or $R = \frac{p_b ot}{0.3|\mathbf{B}|q}$, with $\mathbf{B} = B_z = 1$ T). The coordinate has been chosen as follow: $z$ is aligned with beam (and tracker) axis, $R$ is the radial distance from the $z$ axis, $\phi$ is the azimuthal angle.

The dimensions have been optimized to maximize the acceptance ($\simeq$20% excluding track quality cuts) to Conversion Electronss while minimizing the number of low energy electrons that intersect the tracker.

The particles that cross the tracker release energy by ionization of gas inside the tubes, and the geometry of the tracker allows to have 3D infomation for each "hit" inside the tracker. The transverse position in determined with the measure of the drift time and has a scale of $\sim 10$ ns. The longitudinal position is determined measuring the time difference between each end of the straw and has a resolution of $\sim 3$ cm. To increase the resolution in longitudinal position it is possible to combine the information of two straws in different planes (near in $z$) and obtain a constraint in longitudinal position. In this case it is called "stereo hit".

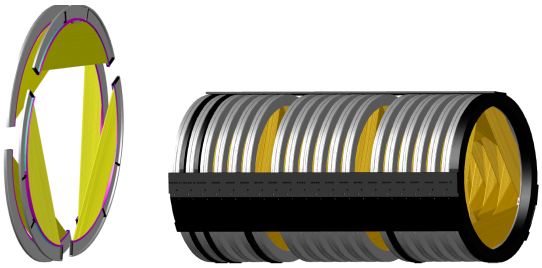

*Figure 1.5: geometry of the entire tracker and the details of the disposition of panels in one plane.*

## 2 Monitoring the muons flux

The incident muon flux on the aluminium target has to be measured and its fluctuation in time has to be evaluated because they can affect the sensitivity of the experiment.

If the number of captured electron is $N$, and $\mathcal{A}$ is the acceptance of the detecor, the number of detected electron will be $n = NR\mathcal{A}$. The Single Event Sensitivity ($SES$) is defined as the factor $R$ when is detected a single electron, so

$$SES = \frac{1}{\mathcal{A}N}. \tag{2.1}$$

So if no events are detected[5], the expected rate of CE events at 90% of confidence level is $R(90\%CL) < 2.3SES$. In presence of background the expected rate is $R(90\%CL) < (2.3 - B) \cdot SES$, where $B$ is the number of background events in accepted window. With the chosen window (electron momentum between 103.95 MeV/c and 105.1 MeV/c) $B \simeq 0.2$, mainly from DIO electrons. In conclusion the variation of muon flux could change the prediction on $B$ and so affect the sensitivity of the experiment (could be evaluated that it is not negligible if the the fluctuation is higher than 10%).

The expected batch by batch fluctuations (from accelerator measurement) are about 50%, so Mu2e need to have a method to monitor the muon flux at batch time scale. The current method to measure the muon flux uses a germanium photodetector placed some meters after the calorimeter (to reduce the acceptance to have a sustainable incident photon flux). These photons are well identified because correspond to the lines of muons nuclear captures in the aluminum target, so the number of photons could be connected to the number of incident muons.

This measurement is very difficult, in particular if is needed a precision higher than 10%. Because of

that and to have a second independent way to cross check the measure is useful to find another method to measure the muon flux.

## 2.1 DIO studies

One alternative method to measure the muon flux is to find a high rate background channel and simply counts the detected particles. If the reconstruction efficiency for this channel is well known it is possible to evaluate the number of particle in production and, by a production model, the number of incident muons.

The first channel candidate for this scope are DIO electrons, because the reconstruction efficiency and the production model are well known. In particular the reconstruction efficiency is approximately:

$$\begin{cases} \varepsilon_{DIO} \sim 0 & p_e < 80 \text{ MeV/c} \\ \varepsilon_{DIO} \sim \text{linear} & 80 < p_e < 95 \text{ MeV/c} \\ \varepsilon_{DIO} \sim 0.1 & 95 < p_e \lesssim 110 \text{ MeV/c}. \end{cases} \tag{2.2}$$

Instead to evaluate the number of DIO produced per incident muon it can be use simply

$$N_{DIO} = (1 - f_{\text{capt}}) f_{\text{stop}} \phi_\mu,$$

where $f_{\text{capt}} \equiv \frac{N_{\text{captured}}}{N_{\text{stopped}}}$.

Weighting the DIO spectrum in figure 1.2 with reconstruction efficiency $\varepsilon_{DIO}$ (using correct normalization) we obtain a reconstructed spectrum that it can be integrated to obtain the number of DIO produced. The figure 2.1 shows the result, and the number of DIO is:

$$\text{DIO total numer} \simeq 9.0 \cdot 10^7 \tag{2.3a}$$

$$\text{DIO number per second} \simeq 4.6. \tag{2.3b}$$

With a rate of $\simeq 5$ Hz is not possible to measure the fluctuation of muon flux at the batch scale (milliseconds). To find another channel with higher rate it is not possible to search in the reconstructed channels because the DIO is the most important background, so is necessary to study and reconstruct a specific channel to perform the measurement.

## 2.2 Proton channel

A good candidate are protons: the expected number of protons from nuclear disintegration is order

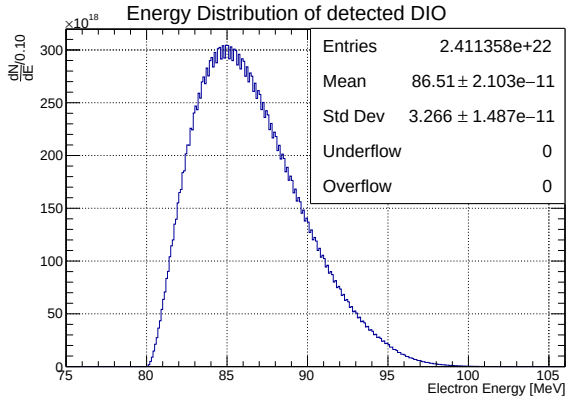


(a) *linear scale*

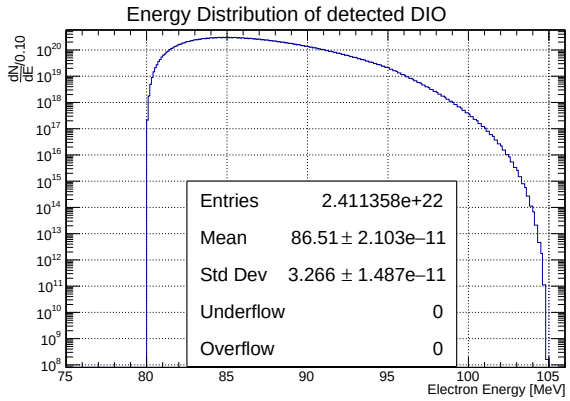


(b) *logarithmic scale, to show the trend near signal window*

*Figure 2.1: Reconstructed spectrum of DIO, using simplified efficiency in equations 2.1*

of $8 \cdot 10^3$/microbunch (a frequency of GHz)[1], but the uncertainty in the production model and in the reconstructed efficiency are expected too big to use the same method proposed for DIO to measure the muon flux.

Anyway it is possible to take advantage of the well known properties of DIO electrons to have an absolute normalization for the number of protons and study only the relative number of produced protons. In details:

- with a measure of the number of DIO detected $N_{DIO}$ for a long time $T_0$ is possible to evaluate the number of incident muons in that time:

  $$N_\mu(T_0) = \varepsilon_{DIO}(1 - f_{\text{capt}} f_{\text{stop}} N_{DIO}(T_0)),$$

  and it gives the absolute scale.

[1] 0.05 protons per muon capture, with $1.62 \cdot 10^5$ captures per microbunch

- make the assumption that the reconstruction efficiency for protons $\varepsilon_p$ (unknown) is simply constant in time, so $\frac{N_p}{N_\mu}(t) \equiv f = \text{const}$ in time.
- from constancy in time is true $f = \frac{N_p(T_0)}{N_\mu(T_0)}$, and $f$ can be evaluated from the measure of protons in $T_0$ and absolute scale.
- measurement of $N_p(t)$ detected at time scale we want (milliseconds or less) and study its fluctuations in time.
- $N_\mu(t) = N_p(t)/f$ by definition

Performing this method, if the reconstructed number of protons is high enough to reach millisecond time scale, the muon flux can be monitored without the use of reconstruction efficiency or production models. Another interesting feature of this method is that use for absolute normalization and for relative measurement two independent and complementary counting: the DIO number is proportional to $(1 - f_{\text{capt}})$, the proton number to $f_{\text{capt}}$. It allows a cross check of the capture fraction, in fact the quantity $\frac{N_p}{N_{DIO}}$ is a function of $f_{\text{capt}}$.

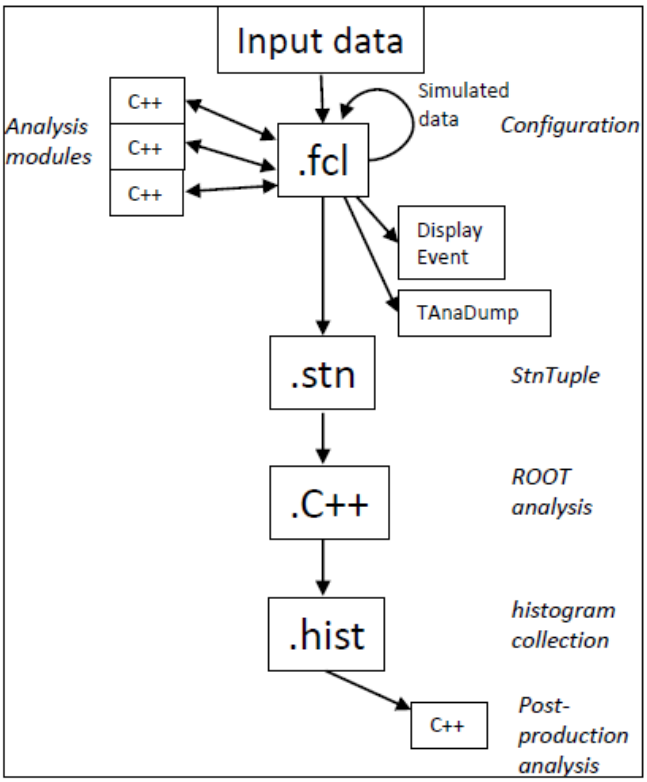


# 3 Proton Reconstruction

## 3.1 Tools of the analysis

The Mu2e offline software works using configuration files (`.fcl` files) that run on `Art` framework. These files call various modules written mainly in `C++` (and use `ROOT` libraries) that actually execute the analysis required in configuration. The configuration files allow to modify deeply the parameter of the analysis without rewriting the whole analysis code.

The output of the run of configuration files are `Stntuple` (`.stn`) files, that contain all the information to perform the final analysis. This analysis is going to be made by another `C++/ROOT` module, that books, builds and analyzes the specific histograms needed for the analysis. This module has as input the `Stntuple` file and as output a collection of `ROOT` histograms.

Eventually, after the production of the histograms other analysis can be made using `ROOT` on the histograms' collection, but this is not recommended because the produced histograms are not data linked as in `ROOT TTree` file, but are "isolated" histograms. So, it is better to perform the analysis directly on `Stntuple` files.

Another two important tools used in the analysis are the Display Event and `TAnaDump` module. The first one can be selected as an alternative output of configuration file and it shows graphically a single event hit distribution in various views (the figure 3.1 shows and describes the details) and it can be useful to understand some properties of the single event and the behavior of the code. The Display Event can be run on multi-event configuration files, but in this case the events have to be scanned manually. `TAnaDump` interactive module that can be used in event-by-event studies (like the Display Event) and it can print on screen detailed information of the single event (hits, tracks, fit, Monte Carlo information...).

The whole work described in this report has been performed on configuration files: it didn't modify the inner code of single `C++` analysis modules but has been only changed the parameter of configuration to reconstruct proton tracks and built correct `Stntuple`. Instead the analysis module that produce and work on the specific histograms has been written specifically for proton tracks analysis.

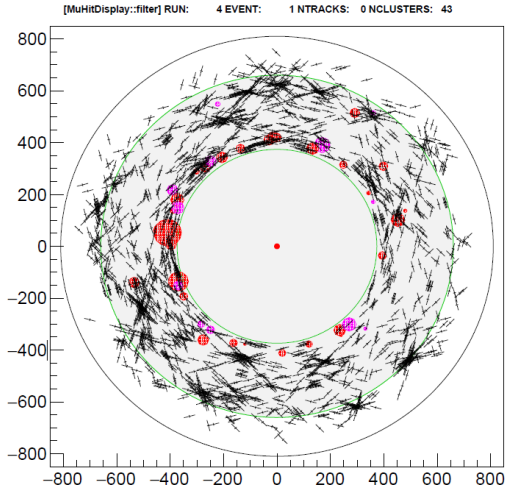


(a) *Tracker+Calorimeter, transverse plane $(R, \phi)$: in green the calorimeter radius, in black the tracker radius, the black lines are MC-truth hits in tracker (proton hits too), the colored circle are calorimeter clusters. The blacker zones corresponds to $\delta$-rays (very small radius of helix, so essentially hits with same $\phi, R$ and different $z$).*

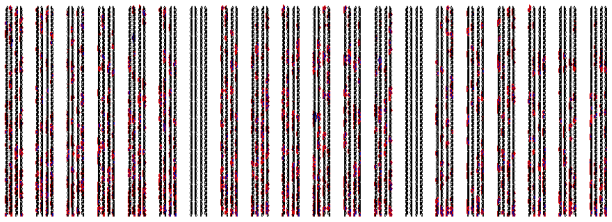

(b) *Tracker, longitudinal plane $(R, Z)$: red dots are MC-truth hits.*

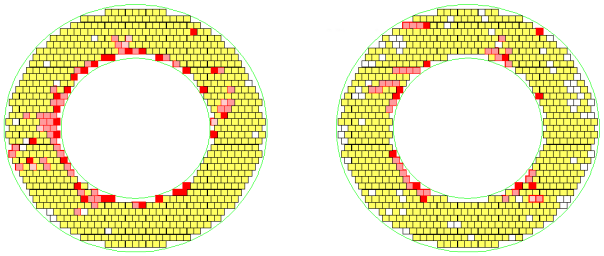

(c) *Calorimeter, 2 disks: red dots are the active crystals from MC-truth.*

*Figure 3.1: An example of display event of nominal background, no tracks are found*

## 3.2 Signal properties

The expected proton signal is very different from the electron signal for the different properties of the particle and its interaction with matter.

The protons from nuclear disintegration are low energy protons and the expected momentum spectrum in production is shown in figure 3.2, so to make some estimate on proton properties it can be considered a proton with $p \simeq 100$ MeV/c.

A 100 MeV/c protons is highly non-relativistic: $\beta \simeq 0.1, \gamma \simeq 1$. For this reason the energy deposition inside the tracker, remembering Bethe-Bloch $\frac{1}{\beta^2}$ trend at low energy, is very bigger than electrons. This is the first and the most important feature of proton signal and it allows to identify and isolate proton hits from other electron-like hits[2]. At tracks level this high energy losses makes the trajectory an helix with a radius that widens in time.

The non-relativistic behavior affects Time Of Flight for protons inside the detector too. An electron that cross the whole tracker has a TOF$\simeq$ 10ns, for protons an estimation could be $\sim 0.1$ $\mu$s, but in most of cases the protons don't cross the tracker and are stopped inside it for the high energy losses. In both cases the time distribution of hits inside the tracker is going to be completely different from electron tracks. Another important point about TOF is that for electrons the time of flight is less than the drift time inside straws ($\sim$ 30 ns), and so essen-

[2] a 100 MeV/c electron has $(1 - \beta) \sim 10^{-5}$ and $\gamma \simeq 12.5$

tially the detector measure the latter. Instead for protons the drift time is negligible.

The low beta make relevant the multiple scattering (so the interaction with nuclei) inside the tracker because $\sqrt{\langle\theta\rangle^2} \sim \frac{1}{\beta^2}$, where $\theta$ is the angle of deviation from a linear trajectory. This effect can change the shape of the proton tracks for lower energy protons from helix, and in all cases makes the track fitting more difficult.

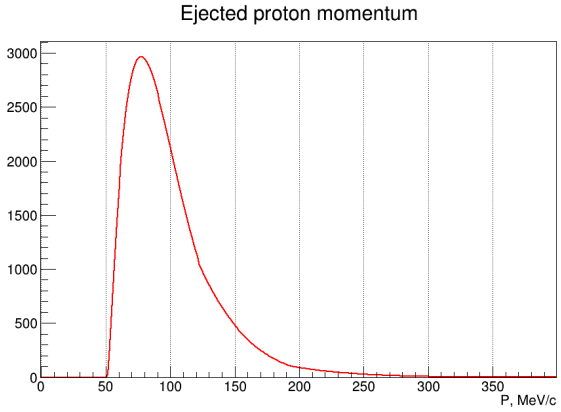


*Figure 3.2: Expected momentum spectrum of protons from nuclear disintegration. On y axis there is an arbitrary scale for flux.*

## 3.3 Previous state of proton reconstruction

The reconstruction code of Mu2e, used on a typical nominal background simulation with the default configuration didn't reconstruct proton tracks. Some studies has been done in proton reconstruction before [1] and they had been obtained some positive results in reconstruction of high energy protons, so the failing point in reconstruction has to come from low energy properties of the proton signal.

Figure 3.1 shows the behavior of proton reconstruction on the nominal background. By Monte Carlo truth it is possible to see proton hits inside the tracker, so the proton detection works property and problems has to be only in reconstruction. The success of reconstruction for high energy protons gives an hint that it is possible to reconstruct protons working only at configuration level.

Actually, by default configuration, protons are rejected from reconstruction algorithm because in common Mu2e analysis they represent a background. As it was said before, a good flag to identify proton hits it is the energy deposition. In figure 3.3 it is possible to see the expected hit energy distribution for protons and electrons. By default the hit energy selection is from 0 keV to 3 keV, that correctly select electrons and reject protons. This selection has to be changed to has a chance to reconstruct proton tracks.

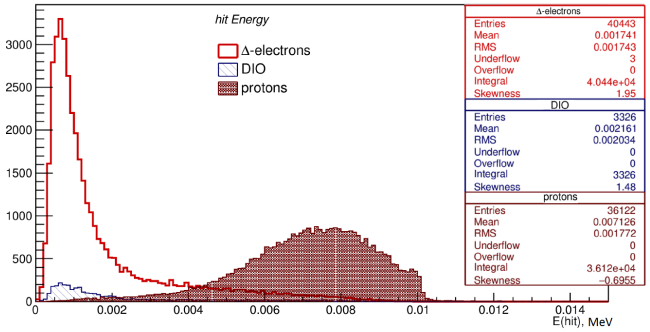


*Figure 3.3: Comparison between energy deposition of single hit for electrons and protons inside the straw tubes. The normalization of y-axis is not relevant and want to show only the relative counting.*

## 3.4 Single proton analysis

From the above discussion the accepted hits energy has to be changed to reconstruct protons. It has been chosen the new range of $E_{\text{hit}} \in [3.5, 11]$ keV to be able to reconstruct most of protons. With this range has been obtained a strong selection for protons: the only[3] hits that pass the selection are proton hits ad a small part of $\delta$-ray hits (discussed below).

With this selection it has been obtained an effective way to isolate proton hits, so it is possible to study why the single proton track is not reconstructed by the reconstruction algorithm. The easier way is to avoid to use the complete background event but to use a "single proton gun", a generator of single proton event of known energy. Then make a debug of reconstruction algorithm step by step on the single track to understand why and where the algorithm fails. During the whole study is convenient to use Monte Carlo truth to understand the behavior of the algorithm.

[3] At this level has not been performed an accurate study of the composition of the sample, so it isn't possible to give the purity of the selection. In section 3.5.1 is going to be discuss this feature of the sample.

The reconstruction algorithm is divided in five steps:

**Step 1: Hit Preparation -** the code flags the hits that have to be used in following steps. The first selection is the on energy deposition (discussed before), than the algorithm defines a fiducial zone inside the tracker (a cut on radius at tracker edge). The studies on hit selection reveal that the momentum of protons has to be bigger than 110 MeV/c to make hits in the tracker because of proton absorber that stops most of protons under this threshold. To make effective studies the "single proton gun" has been set to 150 MeV/c.
The studies on energy selection reveal that a non negligible number of $\delta$-rays produced by protons pass the selection because have enough energy, and it is necessary to study the spatial distribution of these hits to reject them (the main difference from proton hits is the momentum of the particle).

**Step 2: Time Peak Finder -** the algorithm searches for set of hits close each other in time and it selects only event with a recognized time peak. Conceptually the algorithm wants to associate one time peak to a single particle that cross the detector, so the width of the peak is linked to TOF of the particle inside the tracker.
Has been necessary to reduce the threshold of minimum number of hits to define a time peak (from 10 to 5) to be able to collect protons stopped inside tracker. The minimum number of hits had been set 10 for electrons to have high quality time peak and work on clearer event but for protons it is not necessary because the proton events are cleared by energy selection.
Another feature that has been changed is the width, from 30 ns to 70 ns for protons, to take account of different TOF.
With this change in configuration the code is able to recognize proton time peak, but in a large number of cases are found 2 peaks per particle. To understand this behavior in figure 3.5 are plotted the time distribution of hits in some events that actually shows two time peak per event: the algorithm finds two different peaks because the some protons pass inside the tracker, then go inside the central hole and then come back inside the tracker. This trajectory divided in two segments of hits the track and the long TOF mislead the Time Peak Finder that recognize two different time peaks (in figure 3.4 is shown the pattern that produce the double peaks).
To solve this problem the width of time peak has been extended to merge the double peaks, but the hit used in a time peak are not marked, so the code repeat the merging for both the time peaks using the entire set of hit so the output result are two cloned time peak. This result may bring to tracks duplicate, and so to a systematic error in proton counting. At configuration level it is not easily solvable, but is easy to reject the duplicates at analysis level, because the duplicate must have same (or very close) time peak, momentum and all the other tracks parameters. For the moment we didn't take care of the double peaks, but the solution of this bad feature is going to be discussed below.
Excluding the double peak problem this step could reach a good efficiency (for step 2 only, up to 70% at 150 Mev/c) and the main limitation that give an upper limit to time peak identification is the number of hit in the time peak (some times the number is too low to recognize a track).

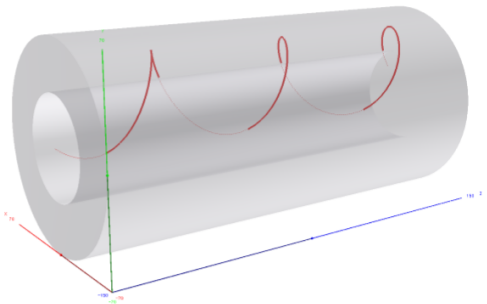

*Figure 3.4: 3D representation of tracker with the pattern of an helix that could produce a double time peak*

**Step 3: Pattern Recognition -** the algorithm studies the spatial distribution of hits to find an helix. It make another selection on hits and give to the seed fit a first pattern to make the fit with smaller errors. To find helix the code searches for triplets of hits to reconstruct the circles, then it finds the center of the circles and at the end it links the centers and finds the helix axis. To find the triples the algorithm has a minimum hit distance and a radius constraint to avoid divergences in radius and center position. Another default constraint is the intersection between the circle and the center of the

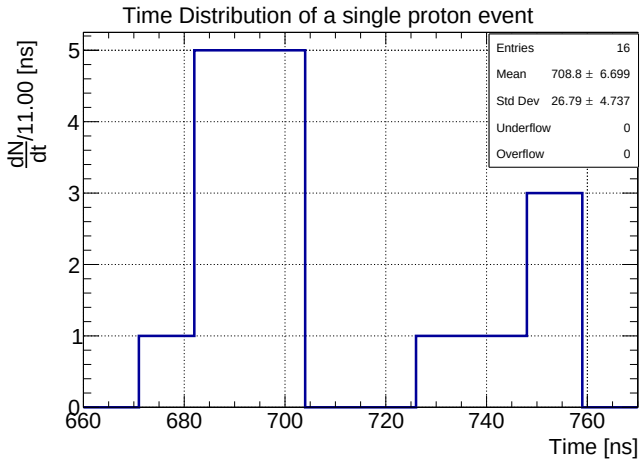


(a) *Time distribution of one single particle*

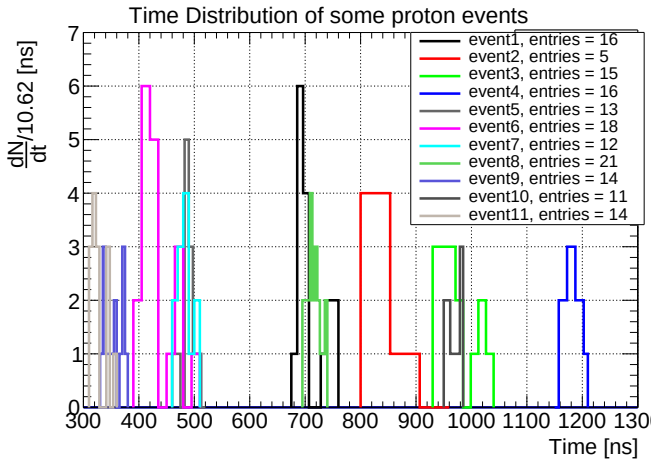


(b) *time distribution of a random set of events*

*Figure 3.5: Time distribution of some proton events. In some cases the distribution shows two peaks per particle, in other cases there is only one peak.*

tracker (so the intersection with the projection of the target) to be sure that the particle came from the aluminium target.
To reconstruct proton helix has been necessary to relax constraints on hit distances and radius (because of different momentum of the particles) and to remove the constraint on the center of the tracker (the multiple scattering inside the absorber makes the protons come different directions, and it seem to not came from the aluminium target).
The efficiency of the pattern recognition is high (for step 3 only, up to 80%) and the main limit are the events with a low number of hits and all the hits very close each other. In these cases the pattern recognition fails for diverges of circle recognition or for failing the distance requirement that has been imposed.

**Step 4: Seed Fit -** in this step the algorithm uses the helix pattern to make a first simplified fit with big ($\sim$ cm) errors on hits and without field and material effects (energy losses). Most of the proton helices has passed this step using default configuration.

**Step 5: Kalman Filter Fit -** the code execute multiple iteration of a Kalman Filter fit using each iteration smaller errors to obtain more accurate helix parameters. The field effect and the material effects are enabled in this step. The left-right ambiguity (ambiguity in decide if the particle has passed to the left or to the right of the wire) is solved minimizing the $\chi^2$ station by station[4].
Using default parameter no tracks passed the Kalman Filter fit (efficiency equal to 0). An operative, non optimized, solution is to request lower hit number in tracks, disable material effects and reduce iterations (from 10 to 3) using larger errors. Doing that the fit converges and finds helices but most of final fit features are disabled.
Still using this relaxed fit the efficiency is low (for step 5 only, under to 35%) and is not possible to increase working at configuration level. If a stronger cut on hit number (from 5 to 20 for example) is made in firsts steps we can move the lack in efficiency in Time Peak Finder and Helix Finder and increase the efficiency of the fitter up to 90% (total efficiency doesn't change).

After the configuration parameter exposed in this section has been changed the reconstruction code turned to be able to reconstruct protons. An example of the result is shown in the Display Event in figure 3.6. The reconstructed momentum is systematically less the the generated one as is expected for energy losses in material.

An accurate optimization of configuration parameter has not been done because the first scope was to understand if the code can reconstruct low energy protons in background events and count them. An increase of efficiency could be not necessary for the muon flux monitoring purpose.

[4]There is an alternative method that minimize the $\chi^2$ globally on the track: it uses the helix axis slope, very sensitive to left-right assignment

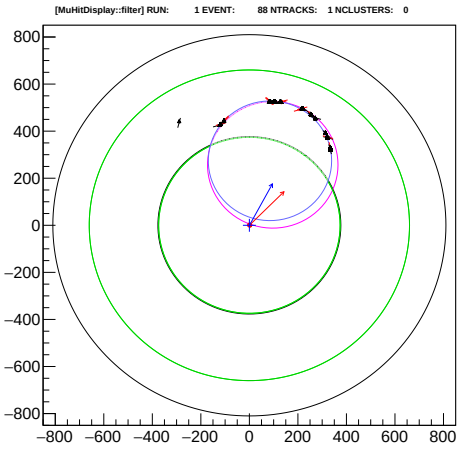


*Figure 3.6: Example of proton reconstruction in transverse plane. The blu line is the fit of first helix circle on the first tracker plane, the pink line is the MC-truth circle on the front of the tracker. The reconstructed momenutm of this proton is* $115 \pm 2$ *MeV/c, the fit has a* $\chi^2/dof \simeq 4.6$ *with 8 dof.*

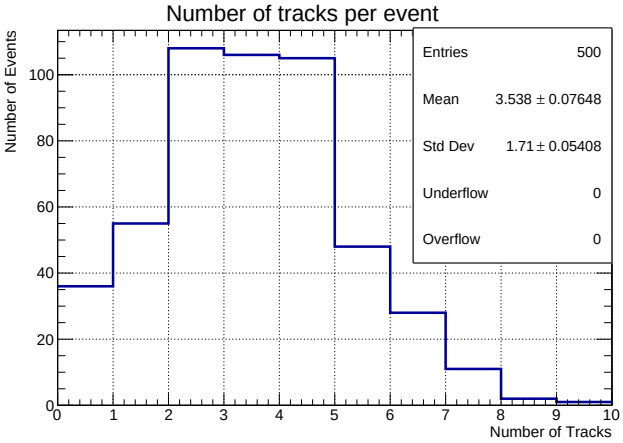


*Figure 3.7: Distribution of number of tracks in the sample of 500 events of nominal background before any quality cuts.*

## 3.5 Background frame reconstruction

After the success in reconstruction in single proton events the following step has been run the reconstruction code configured for proton on nominal background events. It has been chosen the background file in reference [3], that contains 500 events (so 500 microbunch). The proton reconstruction works property on the nominal background events and are found some tracks per event. The figure 3.8 shows an example of the reconstruction in the event display, instead the figure 3.7 shows the distribution of the number of tracks in the whole sample of events.

To evaluate property the number of reconstructed proton is necessary to make some quality cut on the sample and study deeper the composition of the reconstructed sample of tracks. The tracks duplicates problem has to be solved at this level too.

The most effective quality cut is a threshold in number of hits per track, in fact during the single proton analysis a lot of inefficiency in reconstruction came from the tracks with a low hit number. To avoid to work on this kind of track has been imposed a threshold of 15 hits, and has been obtained the distribution in figure **??**

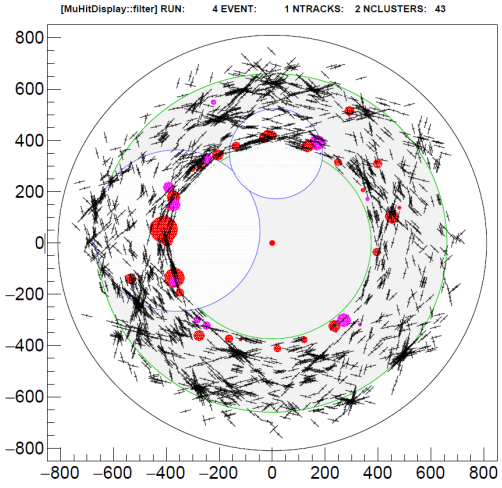


*Figure 3.8: An example of the reconstruction of two proton tracks inside a nominal background event. The blue line is the fit of the circle in the first plane of the tracker.*

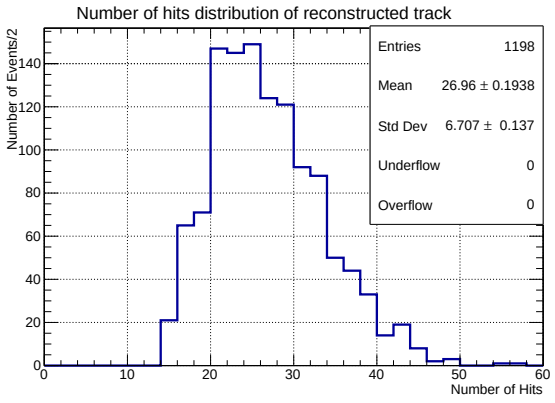


*Figure 3.9: The quality cut removed the problematic left tail of the distribution, without modify the main shape of the distribution*

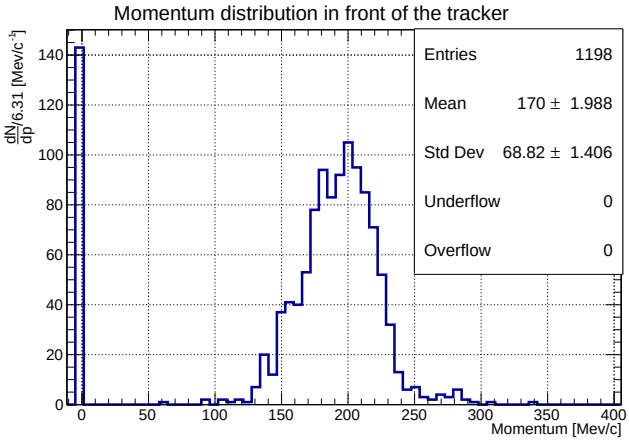


(a) *the main distribution $p_{front}$ has a reasonable shape and shows the deuteron spike in $-1$ bin*

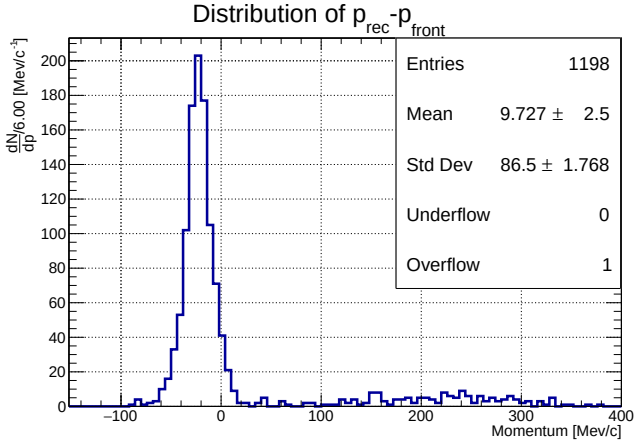


(b) *the main distribution can be fitted with a gaussian obtain a $\chi^2/dof \simeq 2$. The deuteron distribution has too few hit to be correctly described, but the higher bins are between 100 and 300 MeV/c like $p_{front}$ distribution of protons, as we expect (protons and deuterons should have very similar momentum distirbution).*

*Figure 3.10: Sample composition analysis by the use of $p_{front}$*

### 3.5.1 Sample composition

Each reconstructed track has an unique "track ID" inside the event that correspond to the ID of the particle that has the most number of hit of the track. Obviously the track ID is a Monte Carlo information that is unknown in real event. From the particle unique ID, using Monte Carlo truth, it is possible to know the kind of particle of the track by the "PDG code" of particles, so it possible to associate a PDG code to each track.

To study the composition of the sample, so the purity of the track reconstruction, it has been used the Monte Carlo truth to match PDG code of each track with proton PDG code. From this analysis it results that the $\simeq$ 89% of the sample are protons and the $\simeq$ 11% are deuterons. This is not surprising because in nuclear disintegration are produced deuterons too[5] and in reconstruction they are totally indistinguishable from protons (charge, energy deposition, momentum distribution...), but for them the assignment of momentum was wrong because of the incorrect assignment of mass.

A good way to display these deuterons tracks it is the use of the variable $p_{\text{front}}$ defined as the momentum of the track in front of the tracker (this in a Monte Carlo variable too). It has been decided to assign a fixed value $(-1)$ to $p_{\text{front}}$ of particles that ad a PDG code different from protons code. The figure 10(a) shows the result, where it easy to notice the deuterons. In particular can be interesting to plot the difference between the assigned $p_{\text{front}}$ and the reconstructed momentum (figure 10(b)): it has a gaussian-like shape with a negative mean as we expected for energy losses inside the tracker. The mean ($\simeq -20$ MeV/c) gives a scale of the energy losses, and the standard deviation ($\simeq$ 18 MeV/c) a rough scale of uncertainty in reconstructed momentum, both reasonable. To the right of the main distribution are present a distirbution that correspond to the deuterons reconstructed momentum shifted by $-1$.

It is important to understand the composition of the sample for the studies of the properties of the protons but for the purpose of muon flux monitoring this information is not relevant: the deuterons can be included and considered as protons because the method uses DIO electron to absolute normalization. The purity studies could be relevant only if there were electrons between proton tracks.

[5] in particular are expected 0.025 deuterons per muon capture

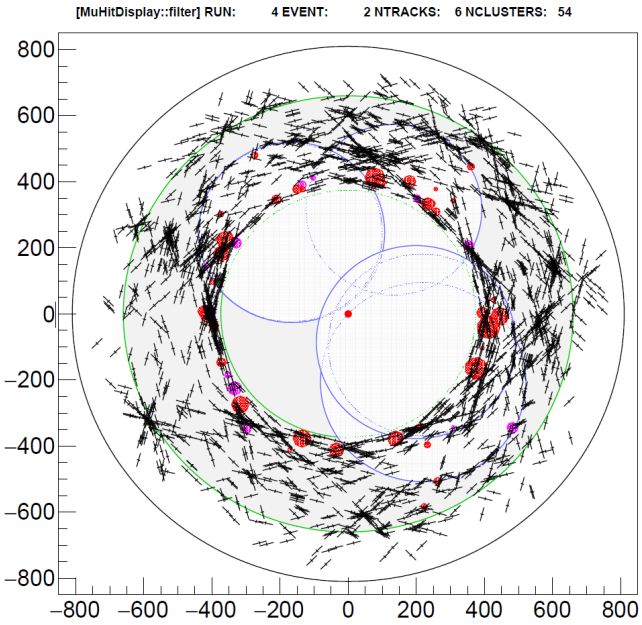


*Figure 3.11: An example of an event with 4 proton and 2 cloned traks shown in event display.*

### 3.5.2 Tracks duplicates

The problem has be fixed at analysis level because it is easier to treat. After the results that are going to be exposed the efficiency of the method allow this faster approach.
The problem is statistically relevant: using Monte Carlo information it is possible to see that 20% of the reconstructed track has in the same event another track with the same unique track ID. This means that the same hits are used for two tracks, so they represent essentially the same particle. So has been found a method to remove the duplicate and maintained the original track.

In figure 3.11 is shown an example where it is possible to notice a typical feature of tracks duplicates: the duplicates has tracks parameters similar (the radius of helix circle in figure) but not completely the same of the true track. So the idea of the fixing method is to find the best track parameters to recognize tracks duplicate, that have to be nearly the same for track and for the duplicate. Than plot the distribution of the difference of these parameter between all the combination of tracks in the same event and hope to see a peak around zero. If it happens, make a cut to remove this peak and use Monte Carlo truth to study the efficiency of the cut.

The chosen parameter are momentum $p$ (one of the main physical parameter of the track) ant time

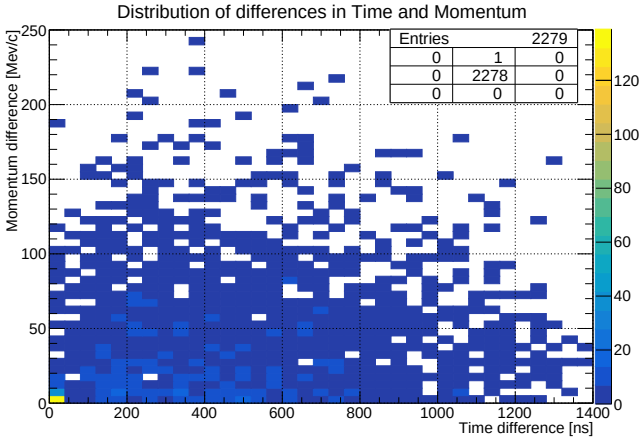


*Figure 3.12: The distribution of all the $\Delta T$ and $\Delta P$ bulit from the 500 events of the sample. The $x-y$ dimension of the peak around 0 is a result of binning*

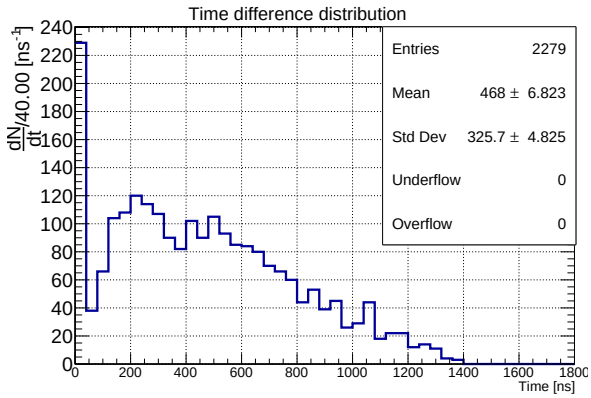


*Figure 3.13: The projection on $\Delta T$ axis of the distribution above, to better show the peak around 0. The $x$ dimension of the peak around 0 is a result of binning.*

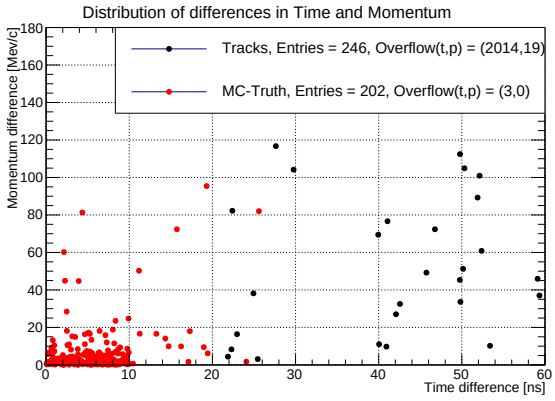


*Figure 3.14: A detail around zero of distribution in figure 3.12, where are evidenced in red the coulples of duplicates using MC-Truth*

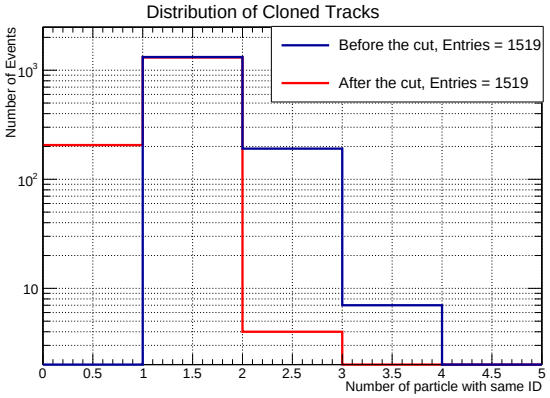


*Figure 3.15: The bin centerd in 1.5 cointain single track, the bin cenetered in 2.5 cointains track with one duplicate, the bin centered in 3.5 cointains track with 2 duplicates and so on. The first bin cointains the track removed after cut. So the cut reduce of 2 order of magnitude the duplicates and doen't remove any single track.*

peak $T$ (the "nearest"[6] parameter to the source of the duplication). So are built the variables $\Delta T$ and $\Delta p$, respectively the absolute difference in time or in momentum between the tracks of the same event. It is possible to see in figure 3.12 that there is a high peak in the first bin of $\Delta T$ and $\Delta p$. Actually, has been understood that the distribution in $\Delta p$ doesn't add information so it has been integrated to obtain the histogram in figure 3.13 that reveal the same anomalous peak around zero.

From the Monte Carlo truth result that most of track duplicates couples has $\Delta T < 20$ ns and in the used sample of event no true tracks couples has $\Delta T < 20$ ns (figure 3.14 shows these distributions), so rejecting one tracks in the couples with $\Delta T < 20$ ns has been obtained a cut with an efficiency $\varepsilon_{\text{dup.cut}} > 97\%$ ($\varepsilon_{\text{dup.cut}}$ defined as number of duplicates removed over the number of total duplicates), without removing true tracks.

In figure 3.15 is shown the situation on duplicates before and after the cut.

## 3.6 Counting of protons

After the fixing of tracks duplicates it is applied has been obtained the distribution in number of tracks in figure 3.16: on average are reconstructed about 3 tracks per event (or per microbunch). With this rate it possible to monitor the flux every millisecond (every $\simeq 600$ microbunches) with a statistical accuracy of 2.3%. So this rate is more than enough to ms time scale or batch-by-batch scale, instead if it will be necessary a monitor of muon flux at micrubunch level the efficiency of reconstruction has to be increased.

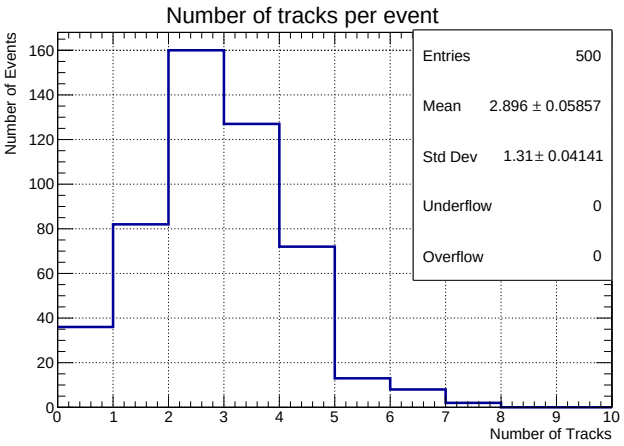


*Figure 3.16: after the cuts the mean is reduced, but remains about 3 protons/microunch, enough for ms scale*

[6] it means that it is the first parameter evaluated after the generation and duplication of the time peak

# 4 Momentum analysis

*Note: most of the analysis and the results that are going to be exposed in this section present some problems. In some cases the problems is clear and it is proposed a solution, in some other cases there are not well understood features in the results. In both cases are presented all the results because they could be useful for further works on proton reconstruction.*

The definition of "reconstructed" track used in previous section it is simply a set of hits that pass all the steps of reconstruction algorithm, associated with the five parameters of the fitted helix and some other parameter of the analysis (from the algorithm, like $\chi^2$, or from physics external information like momentum).

To understand if the reconstruction algorithm is working property is fundamental to understand if the physical property of the tracks correspond to the physical properties of the generated particle. One of the most interesting physical property of the track is the momentum and to make of a complete analysis of that is used a "flat generator": has been generated proton with a flat a distribution in momentum in a wide momentum range (from 70 to 420 MeV/c)[7], then has been performed the analysis on this distribution to understand the behavior of the reconstruction algorithm in whole momentum spectrum. The result is compared step by step with the distribution obtained from the reconstruction of background events.

Before analyze the two momentum distributions could be useful two compare the $\chi^2$/dof distribution of reconstructed tracks. In figure 4.1 it is possible to see that the two distributions have quite the same behavior (shape, mean, standard deviation), it means that the tracking algorithm works in the same way for the to sample of protons in spite of different momentum distribution in production. This reveals a certain robustness of reconstruction algorithm and it confirms that is convenient to use the flat generator to perform momentum analysis.

On the other hand the two $\chi^2$ distribution are both peaked in 2, that reveal an incorrect assignment of errors in fit. A naive interpretation could be a underestimation of errors, and a try of enlarging errors of a $\sqrt{2}$ factor has been done, but it didn't produce the expected results in $\chi^2$ distribution. Probably this behavior is the result of the not well optimized procedure for proton fitting that it has been used. In fact most of features of complete Kalman Filter Fit has been disabled to obtain these results instead they have to be property implemented for protons and enabled. Obviously it can't be done at configuration level, but it needs to work directly on fitting modules. This goes out of the purpose of this work but it is certainly a necessary job to improve proton tracking.

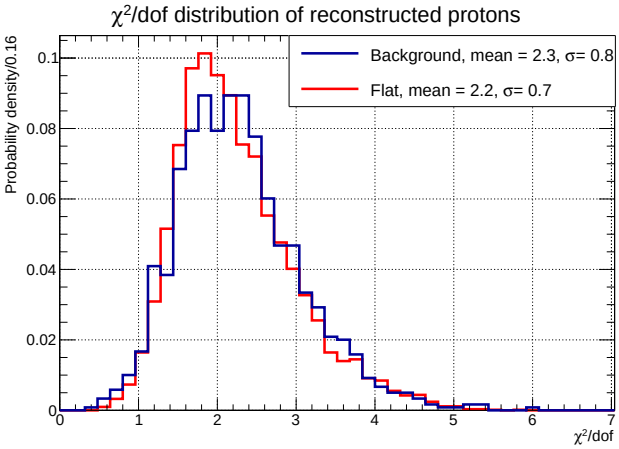


*Figure 4.1: Comparison between $\chi^2$/dof distributions of reconstructed tracks from flat production and from background frame. They have the same behavior but both peak on 2.*

The momentum distributions is shown in figure 4.2: the two distributions are quite similar in mean and standard deviations, but the distribution of reconstructed proton from flat momentum distribution has a bigger right tail. This tail presents a shape that may hide a unsuspected bump around 270 MeV/c. In the distribution from background frame this feature is less evident, but is not possible to exclude that.

Understood that the behavior of the reconstruction of protons from the flat generator spectrum is quite the same of the protons from background frame it is possible to try to use the flat generator go back to momentum distribution in production of the nominal background (the input momentum distribution of protons inside the Monte Carlo of the background frame). This check it is important to understand the lacks and the possible errors in reconstruction.

[7] this range has been chosen looking at the reconstructed momentum distribution from background frame

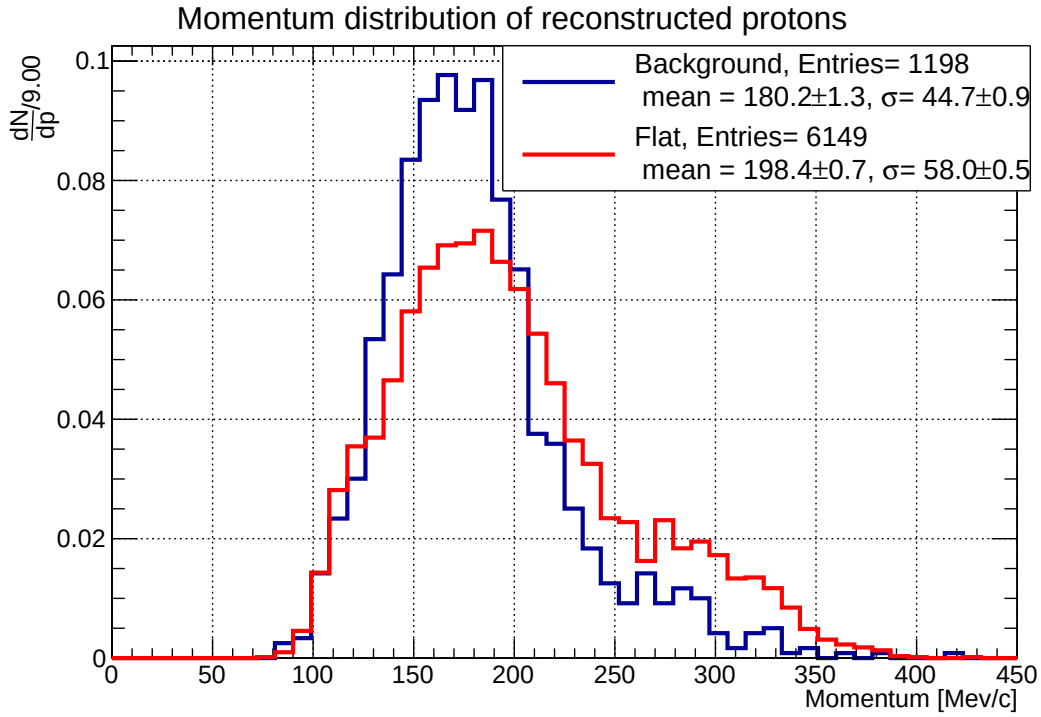


*Figure 4.2: Comparison between the reconstructed momentum bistribution from background frame and from flat generator, correctly normlized. On the right notice the probabile bump not understood*

## 4.1 Deconvolution of the input momentum distribution

To go back to the input momentum distribution is necessary to apply a naive method of unfolding. The known distribution are $N(p)$ the momentum distribution of proton from flat producer at production, $R(p)$ the reconstructed momentum distribution of proton from flat producer and $R'(p)$ the reconstructed momentum distribution of proton from background frame. The purpose is to obtain $N'(p)$, the momentum distribution of proton from background frame at production. The unfolding method has been used is the following:

- Bin the distribution $R(p)$ to obtain $n$ slices $R_i(p)$ with $i = 1, 2 \dots n$. In figure 4.3 is shown the distributions of reconstructed and generated momentum studied to optimize the binning.

- For each reconstructed momentum slice $R_i(p)$, using the Monte Carlo truth go back to the correspondent distribution $N_i(p)$. Notice that a reconstructed bin $R_i(p)$ do not correspond to a single bin of the distribution $N(p)$ but gives a not trivial distribution $N_i(p)$[8].

- Bin the distribution of reconstructed momentum from frame background $R'(p)$ too and evaluate, bin per bin the weights $W_i(p) \equiv \frac{R'_i(p)}{R(p)}$.

- Correct the distributions $N_i(p)$ using the evaluated weights obtaining the correspondents distributions $N'_i(p) = W_i(p)N_i(p)$, that represents the sets of $\{N_i(p)\}$ for protons from background frame.

- Build the distribution $N'(p)$ as a sum of the slices $N'_i(p)$

The figure 4.4 explains graphically the deconvolution method used in the analysis. The figure 4.5 shows the result of deconvolution procedure and compare this result with the Monte Carlo distribution of momentum of generated protons in background frame. The two distributions have the same qualitative shape and the same width but the peak

[8] the "reconstruction" operation is not a function in mathematical sense but energy losses and reconstruction efficiency are convoluted with the input momentum spectrum

of two distribution is shifted of $\sim 40$ MeV/c. There are two probable sources of error: the disabled features of track fitting (in particular energy losses can shift the distribution) and the complete ignorance of the reconstruction efficiency that affecting both flat producer and background frame and so is not completely included in the weighting of the $N_i(p)$ distributions. Further studies have to be done in this direction. After the fixing of these known problems the method could be improved with some iterations: after the first deconvolution, the obtained $N'(p)$ distribution can be used as the new $N(p)$, so as "generator" of protons with that spectrum. Then the deconvolution method should be used on the old $R'(p)$ distribution but with new $N(p)$, $R(p)$. There has not been done studies about this iteration method, so the convergence has not been demonstrated.

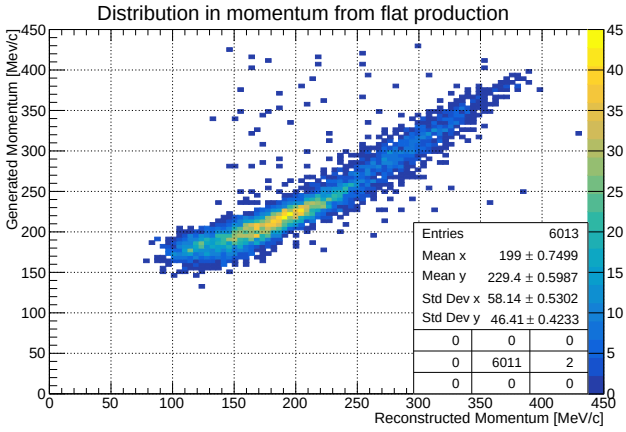


*Figure 4.3: The $N_i(p)$ distributions are obtained slicing vertically this 2D histogram. Notice the not trivial correlation between the distribution of generated and reconstructed momentum*

# 5 Conclusions

The studies that has been done on the reconstruction code of Mu2e have been shown that it can reconstruct protons with some changes at configuration level only, to reproduce the features of proton signal inside the Mu2e tracker.

In nominal background events, at current efficiency, it is possible to reconstruct about 3 protons per microbunch. This results gives an alternative method to monitor the muon flux intensity and to measure its fluctuations at millisecond scale (under batch-to-batch level).

The composition of the reconstructed tracks has been studied and they are 91% protons and 11% of deuterons. This impurity doesn't affect in any way the monitoring efficiency.

The momentum distribution of reconstructed protons has been reconstructed and has been done some studies on the deconvolution of input spectrum of protons. The cross check that has been done in this part of the analysis didn't reveal critical problems in the behavior of reconstruction algorithm.

There are some point that need more intensive studies to be completed. The fitting algorithm has to be optimized for protons and the $\chi^2$ distribution has to be improved. It is necessary to study and optimize the reconstruction efficiency. It is necessary to make a quantitative study on muon flux and its fluctuations. Could be useful to continue the studies on deconvolution method to obtain proton momentum distribution at production level.

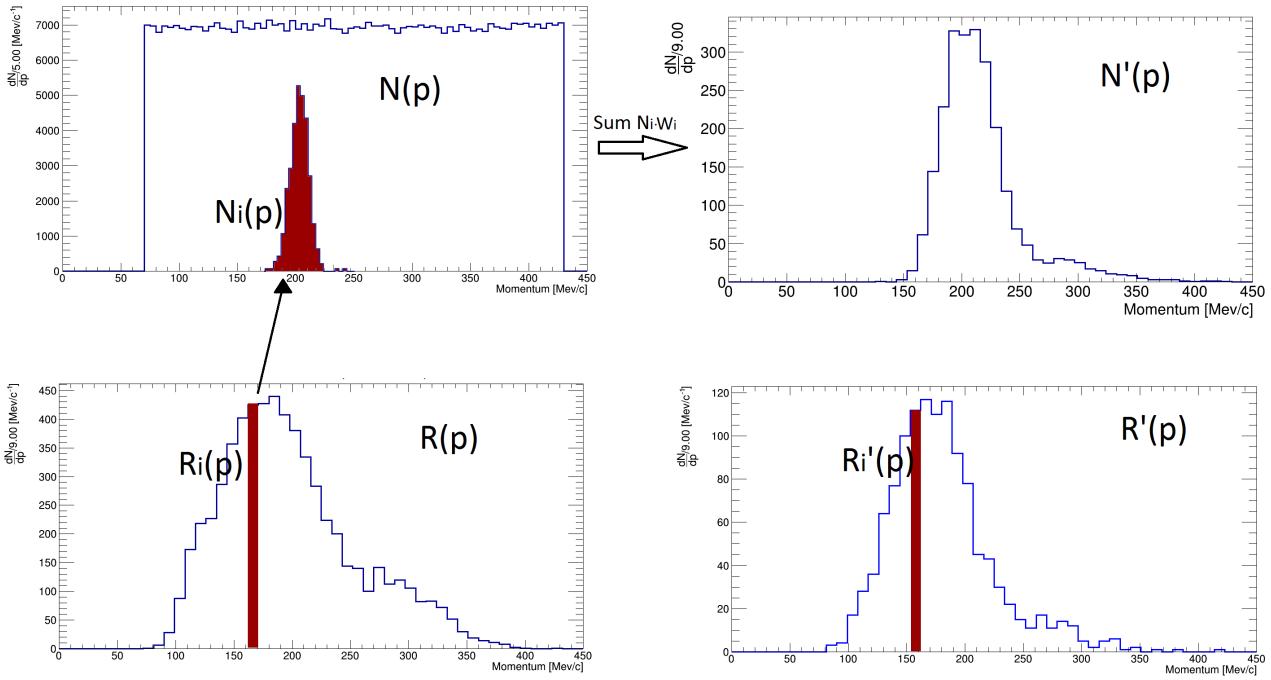


*Figure 4.4: The notations are the same used in the main text. The red zones represent the behaviour of a single slice: in bottom-left histogram the red is the bin $R_i(p)$, in the top-left the correspondent distribution $N_i(p)$ (true shape but not in scale), in the bottom-right the corresponend $R'_i(p)$ used to weight. $N_i(p)$*

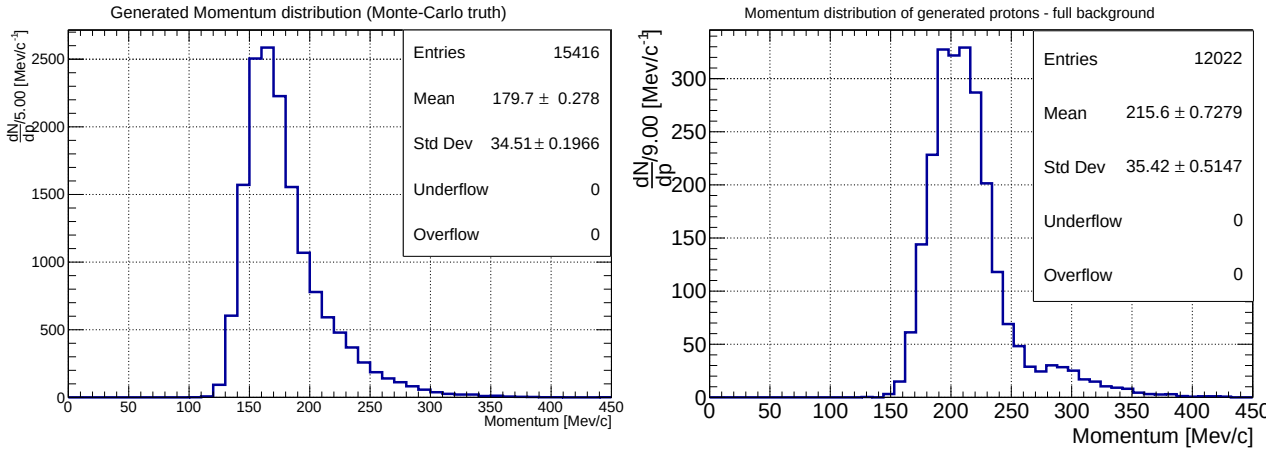


(a) (b)

*Figure 4.5: The results of the deconvolution method to reconstruct the generated momentum distribution of prodons in background frame and the comparison with the real input distribution. Notice that the generated momentum distribution from MC-truth has a left-shape different from the distribution of figure 3.2, in fact there are some not removable filters in Mu2e framework.*

# A Appendix: Reconstruction Efficiency

Using the flat generator has been done some preliminary studies on reconstruction efficiency, but the results are largely not explained so it is possible that the procedure contains bugs.
The efficiency is defined, by the use of flat producer, bin per bin as [9]:

$$\varepsilon(p) = \frac{N_{rec}(p)}{N_{prod}} \pm \frac{1}{N_{prod}}\sqrt{N_{rec}(p)(1-\varepsilon(p))}$$

where $N_{gen}$ is the number of events produced in the bin, $N_{rec}$ is the integral of reconstructed proton momentum distribution corresponding to the generated bin. The result is shown in figure A.1. The trend under 250 MeV/c is reasonable with the property of the detector: $\varepsilon = 0$ under the threshold given by the proton absorber, then a quick increase, a very small range with high efficiency and a slower decrease for tracker geometry. Instead the bump at 300 MeV/c is unexpected and not understood. One interpretation is the following: when protons has sufficient momentum to make 3 segment of hits inside the detector (so 3 loops of the helix) is easier for the algorithm to reconstruct them and the efficiency locally increase. No studies has been done to confirm it, so the interpretation could be totally wrong.

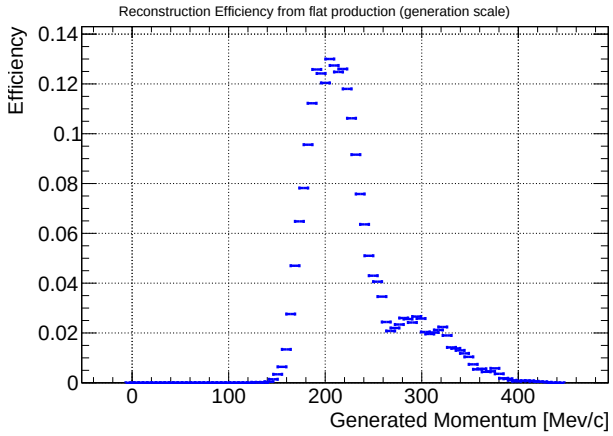


*Figure A.1: preliminary result of reconstruction efficiency: reasonable shape under 250 MeV/c but the bump at 300 MeV/c in completely not understood*

[9] this error formula come from the error propagation using as independent variables $N_{rec}$ and $N_{prod} - N_{rec}$, otherwise there is a correlation between numerator and denominator of the efficiency

# References

[1] D. Brown. *Track Findind in Background Frame.* Mu2e Document 7439-v1. 18 May 2016.

[2] Mu2e Collaboration. *Mu2e Technical Design Report.* Fermi National Accelerator Laboratory Batavia, IL 60510. October 2014.

[3] Mu2e Collaboration. */pnfs/mu2e/tape/phy-sim/sim/mu2e/cd3-detmix-cut/v566b/art/cc/1c/sim.mu2e.cd3-detmix-cut.v566b.000004_00000000.art.* URL: `http://mu2e.fnal.gov/atwork/workgroups/BackgroundWG/cd3-samples/mixp2-nominal-cut.txt`.

[4] A. Czarnecki, X. Garcia i Tormo, and W. Marciano. "Muon decay in orbit: spectrum of high-energy electrons". In: *Physical Review* D84 013006 (2011).

[5] G. J. Feldman and R. D. Counsins. "A Unified Approach to the Classical Statistical Analysis of Small Signals". In: *Physical Review* D57 (1998).

[6] M. Lifshitz and P. Singer. "Nuclear excitation function and particle emission from complex nuclei following muon capture". In: *Physical Review* C22 (1980).

[7] T. Radicioni. *Mu2e tracker momentum calibration using* $\mu^- \to e^-\overline{\nu}_e\nu_\mu$. October 2015.